



HAL
open science

Digital control for disturbance string stability via a mesoscopic approach and redundant macroscopic measurements

Pietro Bonsanto, Mattia Mattioni, Alessio Iovine, Elena De Santis, Maria
Domenica Di Benedetto

► To cite this version:

Pietro Bonsanto, Mattia Mattioni, Alessio Iovine, Elena De Santis, Maria Domenica Di Benedetto. Digital control for disturbance string stability via a mesoscopic approach and redundant macroscopic measurements. 2025. <hal-05249137>

HAL Id: hal-05249137

<https://centralesupelec.hal.science/hal-05249137v1>

Preprint submitted on 11 Sep 2025

HAL is a multi-disciplinary open access archive for the deposit and dissemination of scientific research documents, whether they are published or not. The documents may come from teaching and research institutions in France or abroad, or from public or private research centers.

L'archive ouverte pluridisciplinaire **HAL**, est destinée au dépôt et à la diffusion de documents scientifiques de niveau recherche, publiés ou non, émanant des établissements d'enseignement et de recherche français ou étrangers, des laboratoires publics ou privés.



HAL Authorization

Digital control for disturbance string stability via a mesoscopic approach and redundant macroscopic measurements

Pietro Bonsanto^{1,2}, Mattia Mattioni³, Alessio Iovine⁴, Elena De Santis¹ and Maria Domenica Di Benedetto¹

Abstract—This paper introduces a novel approach for controlling heterogeneous vehicle platoons with connected autonomous vehicles using digital controllers and macroscopic information sharing. The proposed method achieves practical and disturbance string stability despite asynchronous measurements, quantization effects, and redundant information exchange, while offering improved robustness against uncertainties and noise. Simulations illustrate the performances of the proposed controller.

Index Terms—Traffic control; Sampled-data control; Autonomous vehicles; String stability; Quantization; Mesoscopic controller; Micro-macro traffic control systems.

I. INTRODUCTION

Today, the rapid development of intelligent infrastructure and vehicles has led to the emergence of advanced control paradigms, aimed at enhancing efficiency and safety [1]–[3]. In this context, the increasing deployment of connected autonomous vehicles (CAVs) equipped with cooperative adaptive cruise controllers (CACC), which are crucial for achieving these objectives, comes with the drawback of added complexity. To address this issue, many existing approaches focus on ensuring String Stability (SS) and Disturbance String Stability (DSS)—the ability of a platoon of vehicles to attenuate motion perturbations while maintaining desired intervehicular distances [4], [5]. Communication plays a pivotal role in achieving these properties, especially in connected vehicle systems.

Recent studies in the literature (see [4]–[6]) have investigated the possibility of ensuring SS through macroscopic information sharing enabled by vehicle-to-infrastructure (V2I) communication. Specifically, it has been demonstrated that SS can be enforced using mesoscopic controllers, which combine microscopic measurements with aggregated macroscopic data collected across the platoon. The type of information leveraged is also critical: besides the conventional

leader-follower model used in prior works [5], decentralized Multiple Predecessor Following (MPF) models [7] offer promising alternatives that maintain satisfactory performance while enhancing decentralization. Most existing approaches (see [8]–[10]) use a tailored macroscopic function, calculated from the lead to the tailing vehicle. In this work, following [7], [11], [12], we adopt the MPF model, where information exchange occurs only among small vehicle clusters, not the entire platoon. As a result, the informative content is reduced compared to the tailored macroscopic approach, potentially affecting the SS property.

Digital controllers have also been shown to address challenges associated with finite precision and potential data losses in digital systems [13], [14]. To mitigate these limitations, sampled-data approaches and quantization techniques have been introduced. On one hand, sampling signals and maintaining piecewise constant control over the sampling period may impact system properties, particularly when sampling periods are large [15], [16]. On the other hand, quantization—building on prior work in [5]—can potentially compromise global stability results, necessitating practical definitions [17]. Furthermore, as highlighted in [18], asynchronous sampling rates between platoon measurements and macroscopic information can influence desired system properties.

This work aims to advance these directions by considering a platoon of heterogeneous vehicles with asynchronous measurements and disturbances under a digital controller while adopting the MPF sharing paradigm for macroscopic information. Within this framework, we introduce a class of local macroscopic functions designed to enhance robustness against uncertainties and noise compared to previous approaches [5]. Specifically, each vehicle receives information related to macroscopic quantities associated with a subset of preceding vehicles. This information is modeled as a function of macroscopic data and supports various scenarios, such as Laplacian-based coupling over a one-to-one structured graph where exchanged information is affected by noise. As a direct result of consensus-based interconnections, this structure ensures string stability while providing intrinsic robustness against uncertainties such as external noise or quantization.

In this context, we define such exchanged information as redundant since each vehicle possesses data from both its immediate neighbors and tailing vehicles, albeit in partially degraded form. Finally, all measured quantities are subject to quantization. Rather than focusing on specific quantizers, we consider a general class to ensure broad applicability across scenarios. The proposed controller is based on a constant spacing policy and enforces disturbance string

Project co-funded by the European Union – Next Generation Eu - under the National Recovery and Resilience Plan (NRRP), Mission 4 Component 1 Investment 4.1 - Decree No. 118 (2nd March 2023) of Italian Ministry of University and Research - Concession Decree No. 2333 (22nd December 2023) of the Italian Ministry of University and Research, Project code D93C23000450005, within the Italian National Program PhD Programme in Autonomous Systems (DAuSy).

*This work was not supported by any organization

¹Università degli Studi dell'Aquila, Via Vetoio - Coppito, 67100 L'Aquila
pietro.bonsanto@student.univaq.it,
elena.desantis@univaq.it,
mariadomenica.dibenedetto@univaq.it

²Polytechnic of Bari, Dept. of Electrical and Information Engineering,
Via Re David 200 70125 Bari-Italy p.bonsanto@phd.poliba.it

³Dipartimento di Ingegneria Informatica, Automatica e Gestionale A. Ruberti (Università degli Studi di Roma La Sapienza); Via Ariosto 25, 00185 Rome, Italy mattioni@diag.uniroma1.it

⁴Laboratoire des Signaux et Systèmes (L2S), CNRS, CentraleSupélec, Université Paris-Saclay; 3 Rue Joliot Curie, 91190 Gif-sur-Yvette, France alessio.iovine@centralesupelec.fr

stability (DSS) and practical string stability (pSS), despite communication non-idealities and redundant or uncertain information caused by quantization. The design employs a simple feedback mechanism with tunable degrees of freedom that enforce DSS and pSS by ensuring a suitably defined gain remains strictly smaller than one.

The rest of the paper is organized as follows. Section II provides the considered models and hypotheses, as well as the problem statement. Section III introduces the main result with respect to the aforementioned spacing policy. Section IV shows the effectiveness of the proposed sampled-data quantized solution in simulations, while Section V outlines concluding remarks.

NOTATIONS AND INSTRUMENTAL DEFINITIONS

\mathbb{C} , \mathbb{N} and \mathbb{R} denote the set of complex, natural and real numbers including 0 respectively. \mathbb{R}^+ denotes the set of positive real numbers. I and 0 denote respectively the identity and zero matrices of suitable dimensions. Given a matrix $A \in \mathbb{R}^{n \times n}$, $\sigma(A) \subset \mathbb{C}$ is its spectrum. For a complex number $\lambda \in \mathbb{C}$, $\text{Re}(\lambda)$ represents its real part. A is said to be Schur if its spectrum is included in the open unit circle of the complex plane (i.e., all its eigenvalues are with norm strictly less than 1 and none is at the origin). $|\cdot| \in \mathbb{R}$ denotes, depending on the argument, either the cardinality of a set \mathcal{S} , the absolute value of a complex number $\lambda \in \mathbb{C}$ or the norm of a matrix. Given a continuous-time signal $w : \mathbb{R}^+ \mapsto \mathbb{R}$ we define $\|w\|^{[0, \bar{t}]} = \sup_{t \in [0, \bar{t}]} |w(t)|$. Accordingly, for a discrete time signal $w_d : \mathbb{N} \mapsto \mathbb{R}$ we define $\|w_d\|^{[0, \bar{k}]} = \sup_{k \in [0, \bar{k}]} |w_d(k)|$. $1_N = \text{col}\{1, \dots, 1\} \in \mathbb{R}^N$ is the vector with all entries being one. By quantizer we mean a piecewise constant function $q : \mathbb{R} \mapsto \mathcal{Q}^l$, where \mathcal{Q}^l is a finite subset of \mathbb{R} . Any quantizer is characterized by the parameters M, μ , respectively the range and the quantization error, such that the following properties hold: if $|x| \leq M \Rightarrow |q(x) - x| \leq \mu$, if $|x| > M \Rightarrow |q(x)| > M - \mu$. In the following, for the sake of compactness, we will denote the shorthand notation $q(x) = x^q$.

II. MODELING AND PROBLEM FORMULATION

A. Microscopic modeling

Let \mathcal{I}_0^N be the set of N vehicles composing a platoon. Each vehicle is described by its longitudinal position, $p_i \in \mathbb{R}^+$, and its longitudinal speed, $0 \leq v_i \leq v_{\max}$, $v_{\max} \in \mathbb{R}^+$, $\forall i \in \mathcal{I}_0^N$. Then, we define the state of the i -th vehicle as $x_i = [p_i \ v_i]^\top$. Without loss of generality, we can consider simplified models, similar to what seen in [19]–[21]. The corresponding dynamical system, representing the platoon, is obtained [19], [20], [22], [23]:

$$\dot{x}_i = \text{col}\{\dot{p}_i, \dot{v}_i\} = \text{col}\{v_i, u_i + \tilde{d}_i\}, \quad i \in \mathcal{I}_0^N, \quad (1)$$

where: $|u_i| \leq u_{\max}$, $u_{\max} \in \mathbb{R}^+$, is the control input of the i -th vehicle, corresponding to the acceleration. In order to describe inter-vehicular interactions, we adopt the leader-follower model (see [24]). For the derived model to include vehicle $i = 0$, we consider the presence of a virtual leader, $i = -1$, that precedes the entire platoon, with dynamical model

$$\dot{x}_{-1} = \text{col}\{\dot{p}_{-1}, \dot{v}_{-1}\} = \text{col}\{v_{-1}, u_{-1} + \tilde{d}_{-1}\} \quad (2)$$

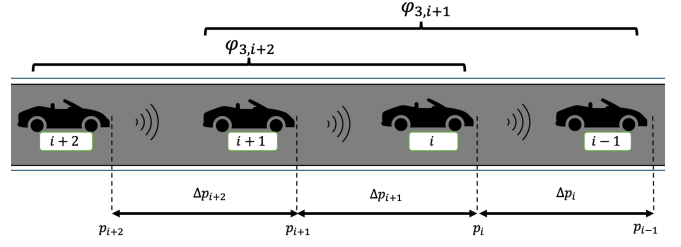


Fig. 1: The reference framework. The curly brackets represent the information flow propagation.

where $u_{-1} = \tilde{d}_{-1} \equiv 0$. Then, the state of each car-following situation between vehicle $i - 1$ and i is defined as

$$\chi_i = \text{col}\{\Delta p_i, \Delta v_i\} = \text{col}\{p_i - p_{i-1}, v_i - v_{i-1}\} \quad (3)$$

Considering a disturbance $z_i \in \mathbb{R}$ acting on the dynamics, the resulting microscopic dynamical model of the i -th car-following pair is

$$\dot{\chi}_i = A\chi_i + B(u_i - u_{i-1} + z_i), \quad i \in \mathcal{I}_0^N \quad (4)$$

and

$$A = \begin{bmatrix} 0 & 1 \\ 0 & 0 \end{bmatrix}, \quad B = \begin{bmatrix} 0 \\ 1 \end{bmatrix}. \quad (5)$$

The disturbance z_i endows errors in the modeling, powertrain dynamics, unexact acceleration cancellations, and predecessor-following interactions, as its structure will be pointed out next. To define the equilibrium point of the platoon, we assume that the virtual leader moves at a constant speed with no disturbance acting over. Thus, the virtual vehicle's speed can be considered as the reference speed of $i = 0$. We adopt a generic spacing policy, denoted $\Delta p_i^r(t_k)$, to be specified later. Then, the equilibrium point for the i th system corresponds to the case where all the vehicles have a distance related to the specific spacing policy adopted, and with same speed, i.e.,

$$\chi_{e,i} = \bar{\chi} := \text{col}\{\Delta p_i^r, 0\}, \quad \text{for all } i \in \mathcal{I}_0^N. \quad (6)$$

From the platoon point of view, we define the lumped state and the lumped equilibrium for $u_{i-1} = 0$ respectively as

$$\chi = \text{col}\{\chi_0, \dots, \chi_N\}, \quad \chi_e = 1_N \otimes \bar{\chi}. \quad (7)$$

B. Macroscopic modeling

We now leverage the influence on each vehicle $j \in \mathcal{I}_0^N$ from both its immediate predecessor and collective platoon interactions, as described in [25, p. 353], by considering the term $z_j \in \mathbb{R}^2$ to describe it. To this goal, we first consider that each vehicle $i \in \mathcal{I}_0^N$ receives partial information on the platoon states. More specifically, for all $i \in \mathcal{I}_0^N$, and for $l \geq 0$, such an information is endowed within the *local* macroscopic function

$$\varphi_{l,i-1}(\sigma_{i-l-1}, \dots, \sigma_{i-1}) : \mathbb{R}^2 \times \dots \times \mathbb{R}^2 \mapsto \mathbb{R}^2 \quad (8)$$

with $\varphi_{l,i-1}(0, \dots, 0) = \text{col}\{0, 0\}$. Then, we define the tailored macroscopic function as

$$\sigma_j = \psi_j(\chi_0, \dots, \chi_j) : \mathbb{R}^2 \times \dots \times \mathbb{R}^2 \rightarrow \mathbb{R}^2 \quad (9)$$

and satisfying $\psi_{i-1}(\chi_{e,1}, \chi_{e,2}, \dots, \chi_{e,i}) = \text{col}\{0, 0\}$. We assume both $\varphi(\cdot)$ and $\psi(\cdot)$ verify, for all $i \in \mathcal{I}_0^N$, for $c_\psi, c_\varphi \in \mathbb{R}^+$

$$|\varphi_{l,i-1}(\sigma_{i-l-1}, \dots, \sigma_{i-1})| \leq c_\varphi \sum_{j=0}^l |\sigma_{i-j-1}| \quad (10)$$

$$|\psi_{i-1}(\chi_0, \dots, \chi_{i-1})| \leq c_\psi \sum_{j=0}^{i-1} |\chi_j|. \quad (11)$$

As aforementioned, we embed such macroscopic function into the disturbance z_i , yielding

$$z_i(t) = d_i(t) + E\varphi_{l,i-1}(t). \quad (12)$$

with $0 < |E| \leq e$ and known bound $e \in \mathbb{R}^+$. In doing so, d_i encompasses modeling errors, powertrain dynamics, and imperfect acceleration cancellations, which are incorporated into the term $d_i(t)$, as well as predecessor-following interactions that are captured by the macroscopic function term $\varphi_{l,i-1}(t)$. Additionally, while still aiming to reflect the physical dynamics of the ahead vehicles, (8) may suffer from decentralization and the consequent loss of information, particularly as the size of the platoon increases and information about the ego vehicles is lost. In pursuit of realism, although (8) continuously affects each vehicle's dynamics over time, we shall assume that it can be measured for control purposes only at certain intermittent time instants.

Remark 2.1: $\varphi(\cdot)$ in (8) is a function of the tailored macroscopic information $\psi_j(\cdot)$ in (9) for $l \geq 0$ and $j \in i-l-1, \dots, i-1$. The particular structure of (8) can be set in different ways depending on the case at hand, allowing it to model and capture distinct phenomena. For instance, as we shall specify later, one can assume that it takes the form of a Laplacian-based coupling among the directly connected l vehicles. This choice, inheriting all properties of Laplacian-based connections [26], will guarantee the desired properties (in terms of SS) while ensuring intrinsic robustness with respect to *dirty* measurements of the tailored macroscopic information $\psi_{i-1}(\cdot)$, as affected in our case by quantization or, more generally, noise. While the former case is evident in the scenario we shall introduce, for the latter, let $l = 0$ for example. Here, (8) might model the fact that $\psi_{i-1}(\cdot)$, acting on each vehicle $i \in \mathcal{I}_0^N$, is affected by an external noise ν_{i-1} ; namely, it is of the form $\varphi_{0,i-1}(\psi_{i-l-1}(\chi_0, \dots, \chi_{i-1})) = \psi_{i-l-1}(\chi_0, \dots, \chi_{i-1} + \nu_{i-1})$.

C. Control Model and Problem Statement

As typical in practice, we assume the input is kept constant during the so-called sampling period. In this respect, we associate to each vehicle $i \in \mathcal{I}_0^N$ the *microscopic* sampling sequence $\Delta_m = \{t_0, t_1, \dots, t_k, \dots\}$ with $t_{k+1} - t_k = T_m, T_m > 0$. At this point, the following assumptions are set.

Assumption 1 (Microscopic Sampling): The input u_i of each vehicle $i \in \mathcal{I}_0^N$ is a piecewise constant signal over the sampling period of length $T_m \geq 0$, namely

$$u(t) = u(t_k) \text{ for all } t \in [t_k, t_{k+1}) \quad (13)$$

with $t_k = kT_m$ and $k \in \mathbb{N}$.

Under the above assumption, the continuous-time model in (4) at all sampling instants $t_k = kT_m$ is equivalently

described by the corresponding sampled-equivalent model, i.e.,

$$\begin{aligned} \chi_i(t_{k+1}) &= A_d \chi_i(t_k) + B_d(u_i(t_k) - u_{i-1}(t_k)) \\ &\quad + f_{\varphi_{l,i-1}}(t_k) + f_{d_i}(t_k) \end{aligned} \quad (14)$$

with

$$\begin{aligned} A_d &= e^{AT_m} = \begin{bmatrix} 1 & T_m \\ 0 & 1 \end{bmatrix}, \\ B_d &= \int_0^{T_m} e^{As} ds B = \begin{bmatrix} T_m \\ \frac{T_m^2}{2} \end{bmatrix}, \\ f_{d_i}(t_k) &= \int_0^{T_m} e^{As} B d_i(t_{k+1} - s) ds \\ f_{\varphi_{l,i-1}}(t_k) &= \int_0^{T_m} e^{As} B E \varphi_{l,i-1}(t_{k+1} - s) ds. \end{aligned}$$

For control purposes, we now define all measures available for control purposes.

Assumption 2 (Microscopic Measurements): Each vehicle $i \in \mathcal{I}_0^N$ measures its corresponding microscopic quantities (i.e., the state x_i , the state x_{i-1} and the input u_{i-1} of its predecessor $i-1 \in \mathcal{I}_0^N$) at all the sampling instants only, which are then subject to quantization.

Furthermore, the second set of measurements available for feedback control pertains to the macroscopic perturbation in (8). We specifically assume these perturbations are measurable by each vehicle only at sparse, intermittent time instants, which generally occur less frequently than those of microscopic measurements (Assumption 2).

Assumption 3 (Macroscopic Sampling): Each vehicle $i \in \mathcal{I}_0^N$ receives the macroscopic information function (8) at all $t_{k^m} \in \Delta_m \{t_{0^m}, t_{1^m}, \dots, t_{k^m}, \dots\} \subseteq \Delta_m$ with corresponding sampling period $T_M := MT_m = t_{k^m+1} - t_{k^m}$ for some $M \in \mathbb{N} \setminus \{0\}$. While being transmitted, such a measure is subject to quantization.

For all $i \in \mathcal{I}_0^N$, let $t_k \in \Delta_m$ denote the microscopic sampling instants and $t_{k^m} \in \Delta_m \subseteq \Delta_m$ represent the macroscopic sampling instants. Similarly, T_m and T_M refer to the microscopic and macroscopic sampling periods, respectively.

Under these assumptions, the control objective is to design a mesoscopic digital controller for tracking based on asynchronous measurements. This approach leverages redundant traffic information while accommodating potential losses of the desired system properties.

In this context, we aim to ensure practical and disturbance string stability for the closed-loop platoon, as defined below.¹

This objective is motivated by the fact that, in the context of SS, as shown in [5], quantization destroys it in the absence of exogenous disturbances. In such cases, only a weaker property—practical string stability, as defined below—can be preserved.

Definition 2.1 (Practical String Stability): For all $i \in \mathcal{I}_0^N$, system (14) is said to be *practically string stable* if there exists $\vartheta_\mu \geq 0$ such that the following conditions hold:

- (i) for all $\varepsilon > 0$ there exists $\alpha_\varepsilon > 0$ such that for all $N \in \mathbb{N}, t_k \in \Delta_m$

$$\max_{i \in \mathcal{I}_0^N} |\chi_i(0) - \chi_{e,i}| < \alpha_\varepsilon \Rightarrow \max_{i \in \mathcal{I}_0^N} |\chi_i(t_k) - \chi_{e,i}| < \varepsilon + \vartheta_\mu; \quad (15)$$

¹For further details on String Stability and Disturbance String Stability, we refer the interested reader to [2], [19], where these concepts are introduced and analyzed in depth.

(ii) the trajectories asymptotically approach the set $\mathcal{B}_{\vartheta_\mu}(\chi_e) = \{\chi \in \mathbb{R}^2 : |\chi - \chi_e| \leq \vartheta_\mu\}$, i.e.

$$\lim_{t_k \rightarrow \infty} |\chi_i(t_k)|_{\mathcal{B}_{\vartheta_\mu}(\chi_e)} = 0. \quad (16)$$

To cope with the eventual presence of exogenous perturbations, the previous definition can be enforced as follows, based on the concept introduced in [21]:

Definition 2.2 (Disturbance String Stability): For all $i \in \mathcal{I}_0^N$, the equilibrium $\chi_{e,i}$ of (14) is said to be *disturbance string stable* if there exist functions β_d of class \mathcal{KL} , ρ_d of class \mathcal{K}_∞ such that, for any initial condition $\chi_i(0)$ and disturbance d_i satisfying

$$\max_{i \in \mathcal{I}_0^N} |\chi_i(0) - \chi_{e,i}| \leq \delta, \quad \max_{i \in \mathcal{I}_0^N} |d_i(t_k)|^{[0,t_k]} < \delta_d \quad (17)$$

the solution $\chi_i(t)$ exists for all $t \geq 0$ and satisfies

$$\max_{i \in \mathcal{I}_0^N} |\chi_i(t_k) - \chi_{e,i}| \leq \beta_d(\max_{i \in \mathcal{I}_0^N} |\chi_i(0) - \chi_{e,i}|, t_k) + \rho_d(\max_{i \in \mathcal{I}_0^N} |d_i|^{[0,t_k]}) \quad \text{for all } N \in \mathbb{N}.$$

The main outcome of this work is to simultaneously ensure DSS in the presence of exogenous perturbations and pSS with respect to quantization as formally stated below, according to their definitions, that is, respectively, Definition 2.2 and Definition 2.1.

Disturbance And Practical String Stability Under Quantization Digital Control Problem (qDSS-DCP). Consider a platoon of vehicles of the form (4) with z_i as in (12), $d_i : \mathbb{R}_{>0} \rightarrow \mathbb{R}$ a bounded disturbance, $\varphi_{l,i-1} : \mathbb{R}^2 \times \dots \times \mathbb{R}^2 \rightarrow \mathbb{R}^2$ satisfying (10). Let Assumptions 1, 2 and 3 hold true and (14) be the sampled-data model associated to (4). Design a mesoscopic sampled-data feedback law of the form

$$u_i(t_k) = u_{i-1}^q(t_k) - K_d \chi_i^q(t_k) - \xi E \varphi_{l,i-1}^q(t_k^m), \quad (18)$$

where $u_{i-1}^q(t_k) := q(u_{i-1}(t_k))$, $\chi_i^q(t_k) = q(\chi_i(t_k))$, $K_d \in \mathbb{R}^{1 \times 2}$, $\xi \in [0, 1)$. making the equilibrium χ_e of the closed-loop platoon qDSS, that is, such that the following holds:

- i) DSS with respect to d_i in the sense of Definition 2.2;
- ii) pSS with respect to quantization in the sense of Definition 2.1. \blacktriangle

III. CONTROL DESIGN

The sampled-data microscopic model (14), together with the controller (18), exhibits the following closed-loop structure

$$\chi_i(t_{k+1}) = F_d \chi_i(t_k) + G_d \varphi_{l,i-1}(t_k^m) + w_i(t_k) + f_{\varphi_{l,i-1}}(t_k) \quad (19)$$

with $F_d = A_d - B_d K_d$, $G_d = -\xi B_d E$ and the term $w_i(t_k)$ defined as

$$\begin{aligned} w_i(t_k) = & f_{d_i}(t_k) + B_d K_d (\chi_i^q(t_k) - \chi_i(t_k)) \\ & + G_d (\varphi_{l,i-1}^q(t_k^m) - \varphi_{l,i-1}(t_k^m)) \\ & + B_d (u_{i-1}^q(t_k) - u_{i-1}(t_k)). \end{aligned} \quad (20)$$

Now we can state the main result, with the proof reported in Appendix.

Theorem 3.1: The qDSS-DCP is solved by the control (18) with K_d and ξ verifying the following conditions:

- 1) the matrix F_d is Schur; è la
- 2) for some $\xi \in [0, 1)$ and $M \in \mathbb{N} \setminus \{0\}$, the parameters

$$\begin{aligned} \gamma(\alpha, \beta, e, \zeta) &= \frac{c \beta b e T_m \zeta}{1 - \alpha} \left(\frac{(1 + \beta \alpha^M)}{(1 - \alpha)} + (1 + \beta) \right) \\ \zeta &= \frac{T_m^2}{2} (2 - \xi) + (M - 1) T_m \end{aligned} \quad (21)$$

verify $\gamma(\alpha, \beta, e, \zeta) \in (0, 1)$ and $\zeta > 0$ with

$$\begin{aligned} \alpha &= \max_{\lambda \in \sigma(F_d)} |\lambda|, \quad \beta = \alpha^{-1} |F_d|, \quad c = c_\varphi c_\psi \\ b &= |B_d| = \frac{T_m}{2} \sqrt{T_m^2 + 4}, \quad e = |E|. \end{aligned}$$

Remark 3.1: Theorem 3.1 provides an estimate for the upper bound of the form (15). The latter in turn depends on the number of vehicles contributing to the construction of the local macroscopic information. The relationship leveraged highlights the fact that the value l does not affect the SS property, which is related to the parameter γ . As one can deduce from the proof of the result, the influence of l on SS is caught by the parameter η in (25) that synthetizes the effect of the redundant quantity on each vehicle i . First, it is easily checked that as $l = 0$, then $(1 + \eta) = (1 - \gamma)^{-1}$, as in [5]. Rather, the more vehicles contributing to the macroscopic information, the bigger the influence of the line, of length l , over the vehicle. This reflects the fact that performances are directly affected by the leveraged information, since the information of the nearest vehicles acts like a noise on the i^{th} vehicle. On the contrary, reduced values for the value l result in better performances, which again is reflected in a tighter bound.

Remark 3.2: We also remark the fact that, if we assume $l = 0$, we have $\varphi_{0,i-1} = \psi_{i-1}(\chi_0, \dots, \chi_{i-1})$ that is, we are using the information of the whole platoon for feedback, we recover the standard tailored macroscopic function. As a consequence, the results recovers the one seen in [5].

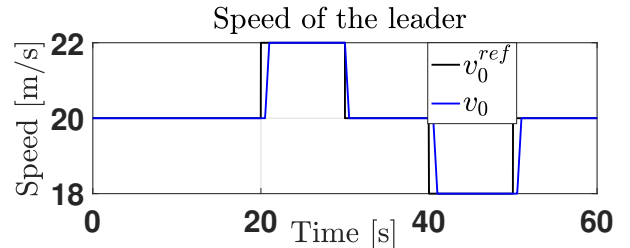


Fig. 2: Speed of the leader and tracked reference.

IV. SIMULATIONS

The proposed digital mesoscopic controller is here verified via numerical simulations in Matlab under realistic settings. We take into consideration a scenario of $N = 9$ vehicles and the leader. The constant desired intervehicular distance is set at $\Delta \bar{p} = 20$ m, and the initial desired speed of the leader is set at 20 m/s. The acceleration of each vehicle is constrained to be such that $|u_i| \leq 5$ m/s². The simulation time is 60 s. For the sake of robustness, we chose a stronger quantizer with quantization noise $\mu = 1$, and we also assume the presence of additive random noise in the tailored macroscopic function. All the vehicles in the platoon are

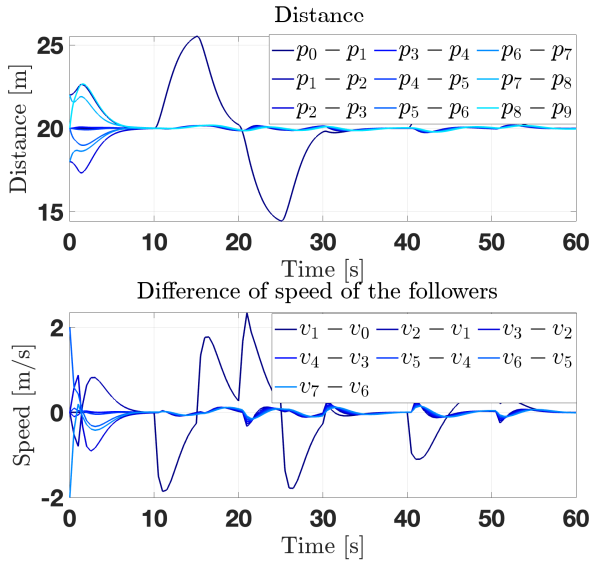


Fig. 3: The distance and velocity difference of each vehicle under the proposed controller with $l = 3$.

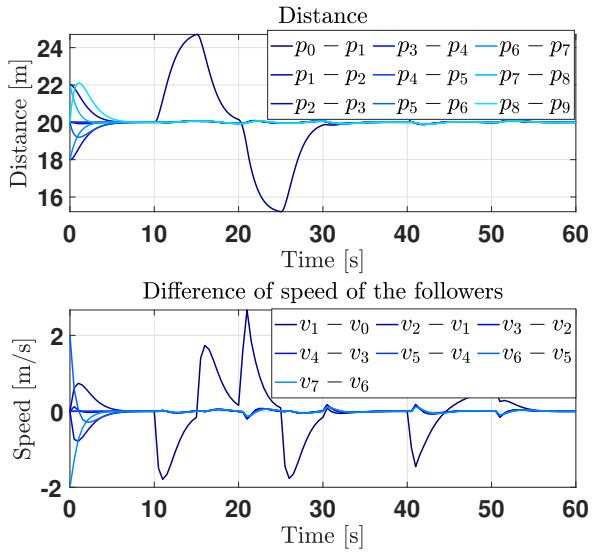
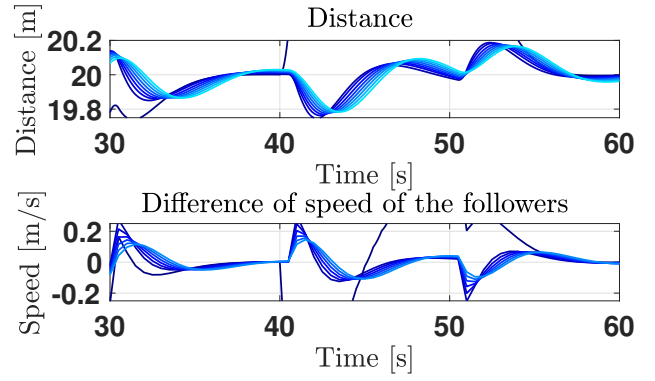


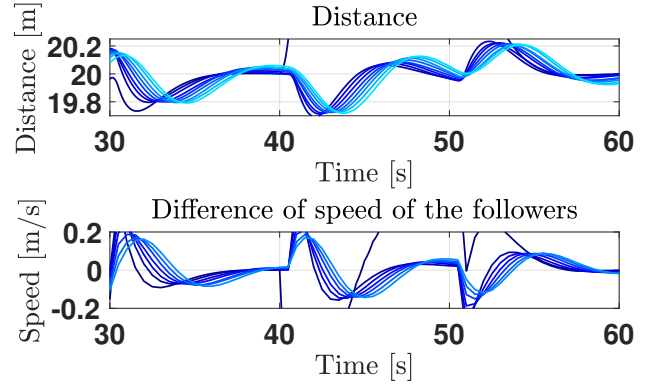
Fig. 4: The distance and velocity difference of each vehicle under the proposed controller with $l = 0$.

initialized with the same initial conditions, i.e., 20 m of distance and 20 m/s speed, except for the fifth and eighth vehicles which have initial distances equal, respectively, to 22 m and 18 m. Following the considerations drawn in the previous sections, we construct the macroscopic function $\psi_i(\cdot)$ as seen in previous works (see [5], [6]). For modeling purposes, from now on we assume the local macroscopic function can be written as a combination of the tailored macroscopic information and the predecessor's macroscopic function as follows:

$$\varphi_{l,i-1}(\sigma_{i-l-1}, \dots, \sigma_{i-1}) = - \sum_{j=1}^l (\sigma_{i-1} - \sigma_{i-j-1}). \quad (22)$$



(a) Zoom of Fig. 3 between $t = 30$ s and $t = 60$ s.

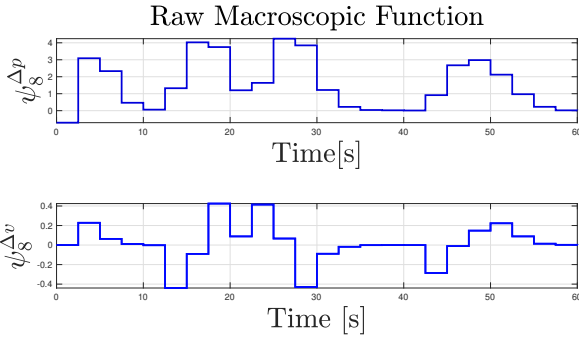


(b) Zoom of Fig. 4 between $t = 30$ s and $t = 60$ s.

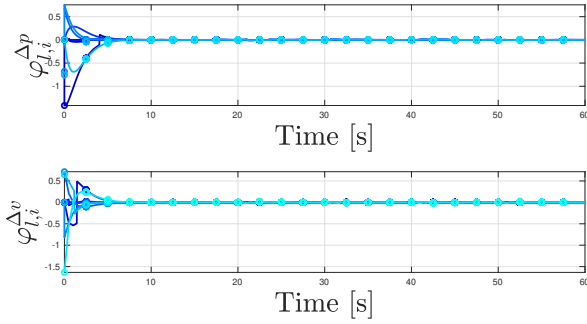
Fig. 5: Comparison between the zoom of distance and speed difference under the proposed controller and under standard tailored macroscopic function.

The function above exhibits a consensus-like structure, as aforementioned is done to ensure robustness to uncertainties on ψ_i . For the considered case, we consider clusters made of $l = 3$ vehicles, such that the macroscopic information gathered for each vehicle entails information of the 3 vehicles ahead only. In the following, the plots for the used macroscopic functions are provided. The quantity acting as a disturbance $\varphi_{l,i-1}$ is represented with the continuous line, together with the values available at the macroscopic sampling instants t_{k^M} , which are represented by "o" in the same plot.

In the numerical setting, hereafter our aim is not only to show the achievement of the SS properties, but to set a discussion regarding the *quality* of the macroscopic information. As highly presented in previous works, as [4]–[6], the use of macroscopic information is a necessary condition for SS in case of constant spacing policy and no information from the platoon's leader. Nevertheless, such works provide the use of the so-called *tailored* macroscopic information, that is, a macroscopic information computed based on the information gathered among all the vehicles of the platoon. Such information is of course as useful as ideal to be available, thus, following our theoretical investigation, in this section we prove that SS can be achieved-with outstanding performances- with the proposed macroscopic information



(a) Constant macroscopic information computed with respect to vehicle $i = 8$.



(b) MPF macroscopic information functions

Fig. 6: The different macroscopic information functions used.

function. The latter also provides robustness towards uncertainties in ψ . Moreover, we also use a *raw* macroscopic function, i.e., computed as in [5] with respect to only the vehicle $i = 8$, that is, $\psi_8(t_k^m)$. The outcome of the choice for the structure of $\varphi_{l,i-1}(\cdot)$ is that the platoon is rendered robust with respect to potential perturbations on the macroscopic function ψ_i , e.g., additive noises of the form $\tilde{\psi} = \psi + d$, as well as with respect to quantization.

In the following, a color scale from dark to light blue is used to represent the pairs of vehicles of the platoon from the head pair $(0, 1)$ (dark blue) to the tail one $(N - 1, N)$ (light blue). The leader of the platoon tracks a piecewise constant reference speed profile $v_{ref}(t)$ that is split as follows: for $t \in [0, 20)s$, $v_{ref} = 20$ m/s, for $t \in [20, 30)s$, $v_{ref} = 22$ m/s, for $t \in [30, 40)s$, $v_{ref} = 20$ m/s, for $t \in [40, 50)s$, $v_{ref} = 18$ m/s, for $t \in [50, 55)s$, $v_{ref} = 20$ m/s. The microscopic sampling time is chosen as $T_m = 0.5$ s and the macroscopic one is $T_M = 2.5$ s, hence, $M = 5$. This choice, together with the one of $K_d = [-0.6183 \quad -1.4181]$ and $R_d = 10^{-3} \begin{bmatrix} 1 & 1 \end{bmatrix}$ results in $\gamma = 0.01$. As far as the exogenous disturbances are concerned, the simulation time is divided into distinct phases: for $t \in [0, 10) \cup [15, 20) \cup [25, 40) \cup [50, 60]$, no disturbance is acting over, i.e., $d_i(t) \equiv 0$ for all $i \in \mathcal{I}_0^{10}$, for $t \in [10, 15)s$, a constant disturbance $d_1(t) = 3$ acts on the first vehicle only, for $t \in [20, 25)s$ a constant disturbance $d_1(t) = -3$ acts on the first vehicle, for $t \in [40, 50)s$ a sinusoidal disturbance is acting on each vehicle of the platoon.

First of all, we notice the leader achieves perfect tracking

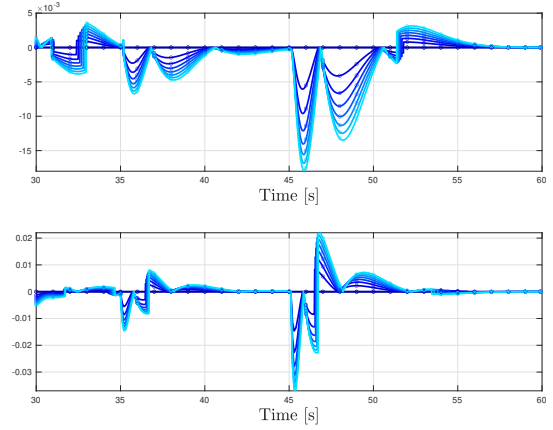


Fig. 7: Zoom of Fig. 6b $t = 30$ s and $t = 60$ s.

of the signal, as noticeable in Fig. 2. The effect of the proposed controller, as noticeable inspecting Fig. 3 is that DSS is achieved: while ensuring the desired intervehicular distance, the disturbances acting do not amplify along the vehicles. This is enforced when comparing the latter figure with Fig. 4, in which we see the effect of the noisy macroscopic function, especially after $t = 10$ s. Indeed, the achievement of DSS is straightforward when inspecting the time instants at which the disturbances start or finish to take place (e.g., $t = 10$ s, $t = 20$ s, $t = 30$ s, $t = 40$ s, $t = 50$ s), since the arising perturbations tend to attenuate. As a second comment, note that in the case with $l = 0$, that is depicted in Fig. 4, also the macroscopic quantity acting as disturbance $\varphi_{l,i-1}(t)$ is attenuated. This is noticeable in the simulation, where the platoon undergoes smaller disturbances. On the other hand, in Fig. 3, the higher value for l implies a scenario in which the disturbances acting are way larger. Regardless, the proposed controller is still able to ensure DSS.

The remarkable effect of the combined use of the two types of macroscopic information is that not only one can achieve DSS and pSS, but also that the chosen structure for the macroscopic function (8) ensures robustness against noise and quantization error. This is remarked when comparing Figs. 5a and 5b. In the latter figure we assume to be in a scenario with tailored macroscopic function computed as in [5], subject to a random noise. The resulting effect in the time window from $t = 30$ s to $t = 60$ s is that the offset is way larger, as we even loose harmonization for the trajectories. The advantage of the leveraged information is thus clearly visible, which outcome, shown in Fig. 5a, is that such effect is highly attenuated, thus proving not only DSS and pSS, but also outstanding performances with an attenuation of uncertainties on ψ_i .

As presented in [5], the effect of the macro info in general is to smoothen the behavior of the distance and velocity for the vehicles; thus, when losing global information of the platoon we notice such harmonization may not be ensured anymore. In this setting, in Fig. 5b the platoon experiences the loss of harmonization of the trajectories right after the changes in the reference ($t = 20, 30, 40, 45$ s), resulting in non-smooth trajectories. The advantage of the proposed

controller lies in the fact of being able to achieve outstanding performances even with redundant and poorer traffic information. Another important effect is the one related to quantization: the aforementioned perturbations arising are the outcome of the mismatch between the quantized past vehicles control actions and the actual ones, which result in the superposition of perturbations. Such perturbations tend then to vanish, proving the pSS behavior. Nonetheless, since the estimate of the offset ϑ_μ is conservative, it may also happen for the trajectories to experience a deviation from the expected equilibrium. Contrarily to previous works, such as [5], where we chose a milder quantizer, here the offset is higher since for the sake of comparison we chose a stronger quantizer. Next we focus on the analysis of the macroscopic information functions, namely Figs. 6-7. More precisely, Fig. 6a shows a *raw* tailored macroscopic function computed with respect to vehicle $i = 8$ and communicated to all the other vehicles, while Figs. 6b and 7 its zoom between $t = 30$ s and $t = 60$ s. Clearly, the information content is higher when the platoon is far from the equilibrium, vanishing when the platoon approaches it. This is noticed when inspecting the behavior at the beginning of the simulation and comparing it when the platoon is at steady state. Another important aspect is the quality of the information: as hinted by the previous sections, the more vehicles contribute to such information, the more noisy the contribution: this is noted when inspecting in particular Fig. 7. On the contrary, the information provided by the raw macroscopic information in Fig. 6a highlights how sampling reduces the informative content.

V. CONCLUSIONS

This work proposes a sampled-data quantized mesoscopic controller achieving practical string stability under quantization effects and disturbance string stability in disturbance-prone environments. By adopting a novel MPF paradigm for macroscopic data integration, the controller operates at the mesoscopic level through asynchronous microscopic-macroscopic measurements, explicitly addressing realistic decentralized scenarios with exogenous disturbances.

Current work addresses time-delayed and noisy measurements, as well as the possibility to predict the macroscopic information to counterbalance the loss due to its asynchronism.

REFERENCES

- [1] R. E. Stern, S. Cui, M. L. Delle Monache, R. Bhadani, M. Bunting, M. Churchill, N. Hamilton, H. Pohlmann, F. Wu, B. Piccoli *et al.*, "Dissipation of stop-and-go waves via control of autonomous vehicles: Field experiments," *Transportation Research Part C: Emerging Technologies*, vol. 89, pp. 205–221, 2018.
- [2] S. Feng, Y. Zhang, S. E. Li, Z. Cao, H. X. Liu, and L. Li, "String stability for vehicular platoon control: Definitions and analysis methods," *Annual Reviews in Control*, vol. 47, pp. 81–97, March 2019.
- [3] D. Swaroop and J. K. Hedrick, "String stability of interconnected systems," *IEEE transactions on automatic control*, vol. 41, no. 3, pp. 349–357, 1996.
- [4] A. Iovine, M. Mattioni, and G. Tedeschi, "Sampled-data string stability for a platoon of heterogeneous vehicles via a mesoscopic approach," in *2024 European Control Conference (ECC)*, 2024, pp. 3364–3369.
- [5] P. Bonsanto, M. Mattioni, A. Iovine, E. De Santis, and M. D. Di Benedetto, "Mesoscopic digital control for practical string stability of vehicular platoons," in *2024 IEEE 63rd Conference on Decision and Control (CDC)*, 2024, pp. 5705–5710.

- [6] M. Mirabilio, A. Iovine, E. De Santis, M. D. Di Benedetto, and G. Pola, "String stability of a vehicular platoon with the use of macroscopic information," *IEEE Transactions on Intelligent Transportation Systems*, vol. 22, no. 9, pp. 5861–5873, 2021.
- [7] E. Abolfazli, B. Besselink, and T. Charalambous, "Minimum time headway in platooning systems under the mpf topology for different wireless communication scenario," *IEEE Transactions on Intelligent Transportation Systems*, vol. 24, no. 4, pp. 4377–4390, 2023.
- [8] M. Mirabilio, A. Iovine, E. De Santis, M. D. Di Benedetto, and G. Pola, "Mesoscopic controller for string stability of platoons with disturbances," *IEEE Transactions on Control of Network Systems*, vol. 9, no. 4, pp. 1754–1766, 2022.
- [9] I. Karafyllis, D. Theodosios, and M. Papageorgiou, "Nonlinear adaptive cruise control of vehicular platoons," *International Journal of Control*, vol. 96, no. 1, pp. 147–169, 2023.
- [10] L. P. Njoua Dongmo, J. Auriol, and A. Iovine, "Smart traffic manager for speed harmonization and stop-and-go waves mitigation dedicated to connected autonomous vehicles," *IEEE Transactions on Control Systems Technology*, pp. 1–16, 2024.
- [11] E. Abolfazli, B. Besselink, and T. Charalambous, "Minimum time headway in platooning systems under the mpf topology for different wireless communication scenario," *IEEE Transactions on Intelligent Transportation Systems*, vol. 24, no. 4, pp. 4377–4390, 2023.
- [12] P. Wijnbergen and B. Besselink, "Existence of decentralized controllers for vehicle platoons: On the role of spacing policies and available measurements," *Systems & Control Letters*, vol. 145, p. 104796, 2020.
- [13] P. Zhu, S. Jin, X. Bu, and Z. Hou, "Distributed data-driven control for a connected heterogeneous vehicle platoon under quantized and switching topologies communication," *IEEE Transactions on Vehicular Technology*, vol. 72, no. 8, pp. 9796–9807, 2023.
- [14] Z. Shen, Y. Liu, Z. Li, and M. H. Nabin, "Cooperative spacing sampled control of vehicle platoon considering undirected topology and analog fading networks," *IEEE Transactions on Intelligent Transportation Systems*, vol. 23, no. 10, pp. 18478–18491, 2022.
- [15] I. Karafyllis and C. Kravaris, "Global stability results for systems under sampled-data control," *International Journal of Robust and Nonlinear Control*, vol. 19, no. 10, pp. 1105–1128, 2009.
- [16] M. Di Ferdinando and P. Pepe, "Sampled-data emulation of dynamic output feedback controllers for nonlinear time-delay systems," *Automatica*, vol. 99, pp. 120–131, 2019.
- [17] M. Di Ferdinando, P. Pepe, and E. Fridman, "Practical stability preservation under sampling, actuation disturbance and measurement noise, for globally lipschitz time-delay systems," in *Accounting for Constraints in Delay Systems*. Springer, 2022, pp. 109–124.
- [18] M. Mattioni and A. Iovine, "Asynchronous sampled-data string stability for a platoon of heterogeneous vehicles via a mesoscopic approach," *IEEE Transactions on Control Systems Technology*, pp. 1–16, 2024.
- [19] D. Swaroop and J. K. Hedrick, "String stability of interconnected systems," *IEEE Transactions on Automatic Control*, vol. 41, no. 3, pp. 349–357, Mar 1996.
- [20] L. Xiao and F. Gao, "Practical string stability of platoon of adaptive cruise control vehicles," *IEEE Transactions on Intelligent Transportation Systems*, vol. 12, no. 4, 2011.
- [21] B. Besselink and K. H. Johansson, "String stability and a delay-based spacing policy for vehicle platoons subject to disturbances," *IEEE Transactions on Automatic Control*, vol. 62, no. 9, pp. 4376–4391, March 2017.
- [22] M. di Bernardo, A. Salvi, and S. Santini, "Distributed consensus strategy for platooning of vehicles in the presence of time-varying heterogeneous communication delays," *IEEE Transactions on Intelligent Transportation Systems*, vol. 16, no. 1, 2015.
- [23] V. Giammarino, S. Baldi, P. Frasca, and M. L. Delle Monache, "Traffic flow on a ring with a single autonomous vehicle: An interconnected stability perspective," *IEEE Transactions on Intelligent Transportation Systems*, vol. 22, no. 8, 2021.
- [24] J. Ploeg, N. van de Wouw, and H. Nijmeijer, " \mathcal{L}_p string stability of cascaded systems application to vehicle platooning," *IEEE Transactions on Control Systems Technology*, vol. 22, no. 2, pp. 786–793, March 2014.
- [25] M. Treiber and A. Kesting, "Traffic flow dynamics," *Traffic Flow Dynamics: Data, Models and Simulation*, Springer-Verlag Berlin Heidelberg, pp. 983–1000, 2013.
- [26] E. Panteley and A. Loria, "Synchronization and dynamic consensus of heterogeneous networked systems," *IEEE Transactions on Automatic Control*, vol. 62, no. 8, pp. 3758–3773, 2017.

APPENDIX

To prove the statements, first note that, when noticing that $t_k = kT_m \in \Delta_m$ and $t_{k^M} = k^M M T_m \in \Delta_M$ and that $t_{k^M} \leq t_k$, one can rewrite

$$k = M k^M + \bar{k}, \quad \bar{k} \in \{0, 1, \dots, M-1\}.$$

Then the explicit dynamics of each vehicle can be rewritten through some computations as

$$\begin{aligned} \chi_i(t_k) = & F_d^k \chi_i(0) + \sum_{j=0}^k F_d^{(k-j-1)} [w_i(t_j) + f_{\varphi_{\sigma, i-1}}(t_j)] \\ & + \mathbf{F}_M \sum_{j=0}^{k^M} F_d^{k^M - (j+1)M} G_d \varphi_{l, i-1}(t_j) \\ & + \mathbf{F}_{\bar{k}} G_d \varphi_{l, i-1}(t_{k^M}) \end{aligned} \quad (23)$$

where $\mathbf{F}_\ell = (I - F_d)^{-1}(I - F_d^\ell)$ for $\ell \in \{M, \bar{k}\}$. At this point, we shall proceed by induction, considering the trajectories of the platoon leader and the first vehicle, and then leverage the properties of the i^{th} vehicle. To this end, for all $\chi_0(0) \in \mathbb{R}^2$, the corresponding trajectories (23) are

$$\chi_0(t_k) = F_d^k \chi_0(0) + \sum_{j=0}^{k-1} F_d^{k-j-1} w_0(t_j).$$

By condition 1), the matrix F_d is Schur stable. Hence, there exist $\beta > 0$ and $\alpha \in (0, 1)$ such that $|F_d^k| \leq \beta \alpha^k$ and therefore

$$|\chi_0(t_k)| \leq \beta \alpha^k |\chi_0(0)| + \frac{\beta}{1-\alpha} \|w_0(t_k)\|^{[0, k]}$$

Consider now $i = 1$ and the trajectories (23). Again, keeping in mind that $|F_d^k| \leq \beta \alpha^k$, one can rewrite

$$\begin{aligned} |\chi_1(t_k)| \leq & \beta \alpha^k |\chi_1(0)| + \frac{\beta}{1-\alpha} \|w_1(t_k)\|^{[0, k]} \\ & + \frac{\beta}{1-\alpha} \|f_{\varphi_{l, 0}}(t_k) + G_d \varphi_{l, 0}(t_{k^M})\|^{[0, k]} \\ \leq & \beta \alpha^k |\chi_1(0)| + \frac{\beta}{1-\alpha} \|w_1(t_k)\|^{[0, k]} \\ & + \frac{\beta b e T_m}{1-\alpha} \left(\frac{T_m^2}{2} (2 - \xi) \right. \\ & + (M-1) T_m \left. \frac{(1+\beta \alpha^M)}{(1-\alpha)} \right) \|\varphi_{l, 0}(t_{k^M})\|^{[0, k^M]} \\ & + \frac{\beta b e T_m}{1-\alpha} \left(\frac{T_m^2}{2} (2 - \xi) \right. \\ & + (M-1) T_m \left. \right) (1 + \beta \alpha^k) \|\varphi_{l, 0}(t_{k^M})\|^{[0, k^M]}. \end{aligned} \quad (24)$$

The latter, combined with (10), (24) and with the definition of (21), yields

$$\begin{aligned} |\chi_1(t_k)| \leq & \beta \alpha^k |\chi_1(0)| + \frac{\beta}{1-\alpha} \|w_1(t_k)\|^{[0, k]} \\ & + \eta \left(|\chi_0(0)| + \frac{\beta}{1-\alpha} \|w_0(t_k)\|^{[0, k]} \right) \\ \leq & \beta (1 + \eta) \max_{l \in \{0, 1\}} \{|\chi_l(0)|\} \\ & + \frac{\beta}{1-\alpha} (1 + \eta) \max_{i \in \{0, 1\}} \{\|w_i(t_k)\|^{[0, k]}\} \end{aligned}$$

with

$$\eta = \gamma \frac{1}{1-\gamma} (1 + \gamma^{N-l-1} (1 - \gamma^l)) \quad (25)$$

Consider now the i^{th} vehicle. the following inequality holds

$$\begin{aligned} |\chi_i(t_k)| \leq & \beta \alpha^k |\chi_i(0)| + \frac{\beta}{1-\alpha} \|w_i(t_k)\|^{[0, k]} \\ & + \frac{\beta}{1-\alpha} \|f_{\varphi_{l, i}}(t_k) + G_d \varphi_{l, i}(t_{k^M})\|^{[0, k]}. \end{aligned}$$

Noticing that $\gamma \in (0, 1)$, using (10) one has

$$\begin{aligned} & \|f_{\varphi_{l, i}}(t_k) + G_d \varphi_{l, i}(t_{k^M})\|^{[0, k]} \\ & \leq b e T_m \zeta \|\varphi_{l, i-1}(s)\|^{[t_{k^M}, t_k]} \\ & \leq b e T_m \zeta c_\varphi \sum_{j=i-l-1}^{i-2} \|\psi_{i-1}(t_{k^M}) - \psi_j(t_{k^M})\|^{[0, k^M]} \\ & \leq b e T_m c_\varphi \zeta \left(c_\psi \sum_{s=0}^{i-1} \|\chi_s(t_{k^M})\|^{[0, k^M]} \right. \\ & \quad \left. + c_\psi \gamma^{i-l-1} \sum_{s=0}^{l-1} \|\chi_s(t_{k^M})\|^{[0, k^M]} \right) \beta \max_{i \in \mathcal{I}_0^N} \{|\chi_i(0)|\} \\ & \leq \frac{\gamma}{1-\gamma} (1 + \gamma^{i-l-1} (1 - \gamma^l)) \beta \max_{i \in \mathcal{I}_0^N} \{|\chi_i(0)|\} \end{aligned}$$

and, at last, when defining the parameters (21), the following inequality holds

$$\begin{aligned} \max_{i \in \mathcal{I}_0^N} \{|\chi_i(t_k)|\} \leq & \beta \max_{i \in \mathcal{I}_0^N} |\chi_i(0)| \\ & + \frac{\beta}{1-\alpha} \max_{i \in \mathcal{I}_0^N} \|w_i(t_k)\|^{[0, k]} + \beta \eta \max_{j \in \mathcal{I}_0^{N-1}} |\chi_j(0)| \\ & + \frac{\beta}{1-\alpha} \eta \max_{i \in \mathcal{I}_0^{N-1}} \|w_i(t_k)\|^{[0, k]}. \end{aligned} \quad (26)$$

Consider now the disturbance (20), which is such that

$$\|w_i(t_k)\|^{[0, k]} \leq 2b\delta_d + b\mu (\kappa + 1 - e\xi(c+1)). \quad (27)$$

Accordingly, combining (26) and (27) with previous arguments one has

$$\begin{aligned} \max_{i \in \mathcal{I}_0^N} \{|\chi_i(t_k)|\} \leq & \beta (1 + \eta) \max_{i \in \mathcal{I}_0^N} \{|\chi_i(0)|\} \\ & + \frac{(1+\eta)\beta b \mu (\kappa + 1 - \xi e(c+1))}{(1-\alpha)} \\ & + \frac{(1+\eta)2b\beta\delta_d}{(1-\alpha)}. \end{aligned} \quad (28)$$

Which, noticing

$$\begin{aligned} \beta b \mu (1 + \eta) (\kappa + 1 - \xi e(c+1)) (1 - \alpha)^{-1} & = \vartheta_\mu \\ 2b\beta (1 + \eta) \delta_d (1 - \alpha)^{-1} & = \vartheta_d \end{aligned}$$

ultimately proves DSS with respect to $d_i(t_k)$ and pSS with respect to μ . \blacktriangle